



ORIGINAL ARTICLE



# Urban Heatwave Dynamics in Lagos State: Evidence from the Analysis of Land Surface Temperature Trends and Land Cover Changes (2000–2022)

Femi Emmanuel Ikuemonisan<sup>1,5</sup> · Samuel Toluwalope Ogunjo<sup>2</sup> · Oluwaseyi Omowunmi Popogbe<sup>3</sup> · Aqil Tariq<sup>4</sup>

Received: 1 March 2025 / Revised: 19 April 2025 / Accepted: 21 April 2025

© King Abdulaziz University and Springer Nature Switzerland AG 2025

## Abstract

Heatwaves are a growing concern in urban environments, exacerbated by rapid urbanization and land cover dynamics. Lagos State has experienced significant land use changes, which have contributed to rising land surface temperatures (LST). To better understand these dynamics, this study investigates the spatiotemporal variability of heatwaves in Lagos State by analyzing satellite-derived temperature data, land cover trends, and urban expansion between 2000 and 2022. Using Moderate Resolution Imaging Spectroradiometer (MODIS) data, LST and land cover data were extracted for 25 locations across Lagos State. The Mann-Kendall trend analysis revealed statistically significant increasing trends in LST at 11 locations, with annual temperature rises ranging from 0.001 °C per year to 0.174 °C per year. Urban expansion, as indicated by MODIS land cover data, showed a 71.2% increase in built-up areas, while vegetative cover declined at a rate of approximately 40 m<sup>2</sup> per year. Coastal areas exhibited lower temperature trends compared to inland urban centres, suggesting the moderating influence of land-sea interactions on heat intensities. The findings reveal the direct impact of urbanization on heatwave intensification and emphasize the urgent need for climate adaptation strategies, including urban greening, improved ventilation corridors, and sustainable land management policies.

## Highlights

- MODIS data reveal that Lagos State experienced a 71.2% increase in built-up areas between 2001 and 2020.
- Land surface temperature increased at 21 out of 25 studied locations, with trends ranging from 0.001 °C per year to 0.174 °C per year, indicating a warming pattern across Lagos State.
- Coastal areas including Epe and Badagry exhibited lower LST values compared to inland urban centers, with LST ranges of 1.62 °C and 4.56 °C, respectively, due to the cooling effects of land-sea breezes.
- Seasonal land surface temperature patterns revealed two peaks annually, with the highest temperatures occurring during the dry season (November–March) and a secondary peak in October, potentially influenced by rainfall.

Femi Emmanuel Ikuemonisan  
femi.ik@yahoo.com

Samuel Toluwalope Ogunjo  
stogunjo@futa.edu.ng

Oluwaseyi Omowunmi Popogbe  
popogbeseyi@gmail.com

Aqil Tariq  
at2139@msstate.edu

<sup>2</sup> Department of Physics, Federal University of Technology, Akure, Nigeria

<sup>3</sup> Department of Economics, Crawford University, Faith City, Igbese, Ogun State, Nigeria

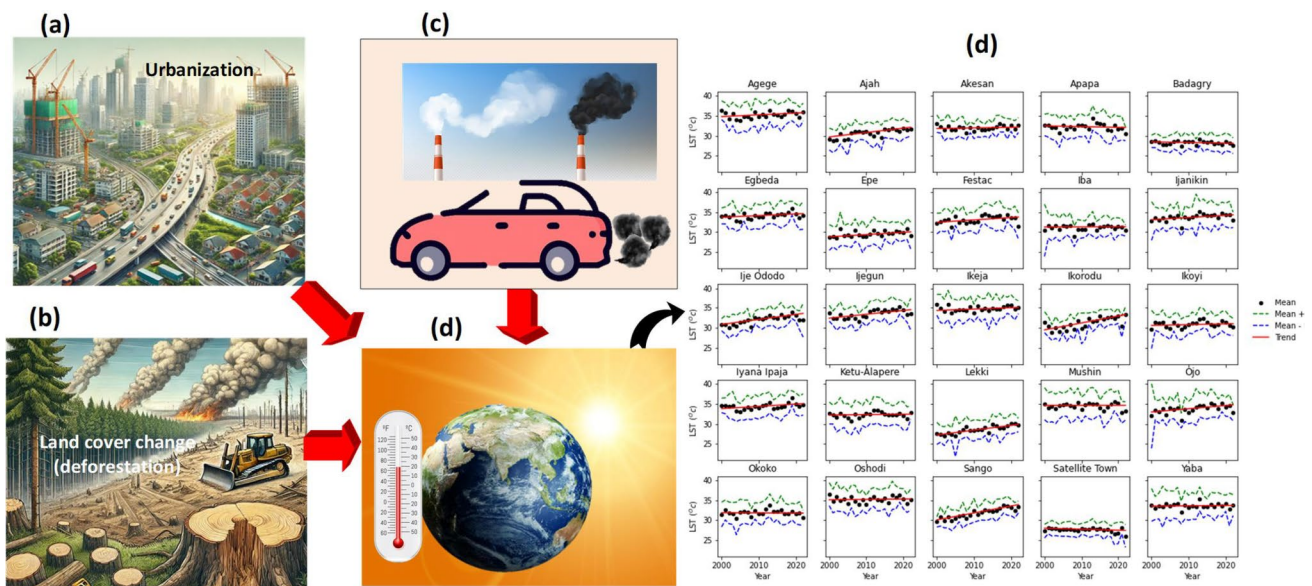
<sup>4</sup> Department of Wildlife, Fisheries and Aquaculture, College of Forest Resources, Mississippi State University, Starkville, MS 39762-9690, USA

<sup>5</sup> Department of Physics, Lagos State University of Education, Oto/Ijanikin, Lagos, Nigeria

<sup>1</sup> Department of Physics (Geophysics Research Group), Lagos State University of Education, Oto/Ijanikin, Lagos, Nigeria

## Graphical Abstract

Urban heatwaves in Lagos State are increasingly shaped by the interaction of natural and anthropogenic factors. The study captures these dynamics through a series of interconnected components, as illustrated in the graphical abstract: (a) an image of urbanization illustrates the rapid expansion of cityscapes, infrastructure development, and population growth, which drive significant increases in LST as natural surfaces are replaced with heat-absorbing materials. These are paired with (b) representations of land cover changes, mainly deforestation, showing the transformation of green spaces and forested areas into built environments, a process that reduces evapotranspiration and exacerbates surface heating. The graphical abstract also includes (c) a depiction of solar radiation, with rays striking the Earth's surface, to illustrate the natural mechanism contributing to global warming and elevated LST. Additionally, (d) emissions from industrial smokestacks and vehicles are shown, representing anthropogenic sources of greenhouse gases that intensify the urban heat island effect. Finally, (e) graphs displaying LST trends over time at some reference locations in Lagos State reveal the spatial and temporal temperature variations, indicating the dynamic heatwave patterns linked to urbanization and land cover changes. Together, these elements form a cohesive representation of the study's findings, revealing the interconnected effects of urbanization, land cover changes, and rising temperatures on urban heatwave dynamics in Lagos State over the two-decade period.



**Keywords** Climate change impacts · Heatwave · Land surface temperature · Urbanization

## 1 Introduction

Heatwaves are prolonged periods of unusually high temperatures and are among the most worrying consequences of climate change in recent decades, given their increasing frequency, intensity, and long duration (Smith et al. 2013; Perkins-Kirkpatrick et al., 2017; Marx et al. 2021). These extreme events pose significant risks to human populations and ecosystems, with urban areas particularly vulnerable due to the exacerbating effects of urban heat islands (UHIs). The UHI phenomenon occurs when built environments, characterized by impervious surfaces, dense infrastructure, and limited vegetation, trap and retain heat. This results in urban areas being significantly warmer than their rural counterparts (Zuo et al. 2015; Zhao et al. 2018; IPCC 2021;

Harmay and Choi 2022). The primary drivers of heatwaves are natural variability in atmospheric circulation patterns and anthropogenic climate change (Wehrli et al. 2019; Jiménez-Esteve et al., 2022). However, in urban areas, these factors interact with local land-use changes and the UHI effect to alter the frequency and intensity of heatwaves. Impervious surfaces such as asphalt and concrete absorb more solar radiation, whereas reduced vegetation diminishes evaporative cooling (Speak et al. 2013; Ren et al. 2024). High-density infrastructure impedes air circulation, creating localized heat pockets that heighten thermal stress during heatwaves (United Nations 2019; Kong et al. 2021; Zou et al. 2021). These conditions often lead to increased energy demands, reduced air quality, and heightened public health risks. These make heatwaves among the deadliest natural

hazards globally, as highlighted by the World Health Organization (WHO, 2022).

The effects of heatwaves are wide-ranging, with significant implications for public health, infrastructure, and ecosystems (Zuo et al. 2015; Cheng et al. 2019). Prolonged exposure to extreme heat increases the risk of heat-related illnesses such as heat exhaustion and heatstroke, particularly among vulnerable groups, including elderly individuals, children, and individuals with preexisting health conditions (Anderson and Bell 2011; Lucas et al. 2014; Leyk et al. 2019; Bouchama et al. 2022). Urban areas with high population densities often experience compound challenges, as limited cooling infrastructure and socioeconomic disparities restrict access to adequate adaptation measures (Fu et al. 2015; Lemonsu et al. 2015). Additionally, heatwaves strain urban infrastructure, causing energy demand to surge, which can overwhelm power grids and lead to outages (McEvoy et al. 2012). The resulting reliance on air conditioning further increases greenhouse gas emissions, propagating a cycle of warming and environmental degradation (Obe et al. 2023).

Lagos State, which comprises Lagos metropolis, Nigeria's most populous city and a rapidly expanding urban center, faces particularly severe impacts from heatwaves (Ogunjo et al. 2023). Rapid urbanization has dramatically altered the city's land cover, replacing natural vegetation with impervious surfaces such as concrete and asphalt, which absorb and retain heat. Between 1984 and 2015, Lagos State experienced a 53% increase in built-up areas and a rise in LST from 0.579 °C to 2.80 °C (Obiefuna et al. 2018). The city's high population density, poor urban planning, and limited green spaces further intensify its vulnerability to heatwaves (Adegun et al. 2015; Merem et al. 2018). With over 20 million residents and projections suggesting that it could become Africa's most populous city by 2050, Lagos State is increasingly at risk of extreme heat events (UN-Habitat 2020). The indiscriminate drilling of boreholes, necessitated by an inadequate public water supply, exacerbates this vulnerability. Excessive groundwater extraction contributes to land subsidence, which worsens flood risks and alters surface conditions, making the land more prone to heat retention (Ikuemonisan and Ozebo 2020; Ikuemonisan et al. 2020). Furthermore, spatial analyses of the UHI effect reveal significant disparities. Low-income communities are disproportionately exposed to higher temperatures due to poor housing quality, inadequate ventilation, and minimal access to cooling infrastructure and green spaces (Degirmenci et al. 2021; Meenar et al. 2023). These communities are also the least equipped to cope with heatwave impacts, highlighting Lagos State's intersection of environmental and social vulnerabilities (Laue et al. 2022).

Research on urban heatwave dynamics has advanced in response to growing concerns about climate change, rapid

urbanization, and environmental degradation, particularly in fast-growing cities across the Global South (Intergovernmental Panel on Climate Change [IPCC] 2021; United Nations Human Settlements Programme [UN-Habitat] 2020). Early studies focused primarily on temperate regions, but with the advent of satellite remote sensing technologies like MODIS and Landsat, researchers can now better assess LST and its relationship with land cover changes in tropical urban areas. Recent work has adopted spatiotemporal approaches to analyze localized heatwave patterns, supported by statistical methods such as the Mann-Kendall trend test to identify long-term warming trends driven by urbanization (Guo et al. 2018; Gadedjisse-Tossou et al. 2021). Yet, despite these advancements, detailed investigations into heatwave variability in Lagos, where urban expansion and vegetation loss have been pronounced over the past two decades (Adegun et al. 2015; Kasim et al. 2022), remain limited. Previous studies in the region have largely examined broad UHI effects (Nwilo et al. 2012), overlooking how land cover dynamics shape localized temperature variations across the city. Most of the existing studies on heatwaves present some limitations that leave room for further study. Most investigations have focused on the broad relationships between urbanization and surface temperatures, often relying on ground-based data collection methods (Ogunjo et al. 2021). While these methods provide valuable localized information, their spatial coverage is insufficient to capture the variability in temperature patterns across Lagos State's vast, densely populated, and rapidly urbanizing landscape. For example, Obiefuna et al. (2018) identified substantial land cover changes and associated increases in LST between 1984 and 2015. Still, they did not consider the spatiotemporal variability of heatwaves in sufficient detail. Similarly, Guo et al. (2022) reported temperature increases of 1.429 °C during the day and 0.563 °C at night per decade, which were influenced by urbanization and climate change. However, their study did not extensively examine localized drivers or the nuanced role of land-use changes. In addition, studies leveraging remote sensing data, although commendable for their broader spatial coverage, often rely on datasets that may no longer fully reflect the current realities of rapidly urbanizing cities like Lagos metropolis. Dissanayake et al. (2018) applied remote sensing techniques to explore the relationship between land use and heatwaves. Still, the land-use data used in their analysis were last acquired in 2013. Given the dynamic and evolving urban landscape of Lagos State, the applicability of their findings to present-day conditions is somewhat limited.

Given the above, there is a need to build upon prior research addressing the spatiotemporal variability of heatwaves in Lagos State, particularly in the context of rapid urbanization, shifting land-use patterns, and the UHI effect.

By incorporating high-resolution satellite-derived temperature data, up-to-date land cover information, and a more detailed analysis of localized urban drivers, we can accurately quantify the spatial and temporal trends of heatwaves in Lagos State. This effort will support targeted urban greening and climate adaptation strategies for Lagos State. Hence, this study uses recent data to address these gaps by leveraging satellite-derived data to investigate the spatio-temporal trends of heatwaves and their underlying drivers at 25 locations in Lagos State. This study utilizes MODIS surface temperature data with a spatial resolution of 1 km and a daily temporal resolution. Additionally, the vegetation indices employed have a spatial resolution of 500 m and an annual temporal resolution. Moreover, the influence of land cover change on heatwave variability is assessed using the MODIS land cover product (MCD12Q1). Through a synthesis of these datasets, this study seeks to enhance understanding of the key drivers of heatwave variability in Lagos State. The findings aim to support the development of targeted adaptation strategies, addressing the increasing vulnerability of urban areas to climate change impacts.

## 2 Methods and Datasets

### 2.1 Study Area

Lagos State is in a vegetated tropical zone and broadly comprises mangrove swamps, rainforests, and freshwater swamps (Ajikah et al. 2023). It experiences a tropical equatorial climate with high rainfall and moderate temperatures (Sojobi et al. 2016). The rainfall pattern is divided into two seasons: the wet and dry seasons. The wet season typically occurs between April and October, with an average annual rainfall of approximately 1600 mm, while the dry season usually spans from November to March (Dissanayake et al. 2018; Emekwuru and Ejohwomu 2023). Lagos State's proximity to the ocean makes it highly vulnerable to rising sea levels and coastal flooding, as highlighted by the IPCC. With a population exceeding 22 million, the city ranks among the most populous urban centers globally, driven by rapid urbanization, migration, and natural population growth (Auwalu and Bello 2023; Opoko and Oluwatayo 2014). This exponential growth, however, has given rise to significant socioeconomic challenges (Okuneye et al. 2016; Osho and Ojumu 2024). Lagos State has many residents living in informal settlements with limited access to essential services, housing, and infrastructure. As the population grows, the loss of green spaces significantly increases, impacting vegetation and exacerbating environmental challenges (Adeyemi and Shackleton 2023; Mensah 2014). The close spacing of housing units in the built-up area and the

extensive use of heat-retaining materials such as concrete and asphalt exacerbate the UHI effect and pose significant environmental and health risks (Ojeh et al. 2016; Emetere 2019).

### 2.2 Land Surface Temperature

To analyse the LST at various locations, we utilized the Moderate Resolution Imaging Spectroradiometer (MODIS) LST product MODIS/006/MOD11 A2 dataset accessed through the Google Earth Engine (GEE). This dataset spans from 2000 to 2022, and provides LST data as 8-day composites, meaning that each value represents the average temperature over 8 days. The dataset has a spatial resolution of 1 km and includes several key bands, such as daytime and nighttime LSTs, quality assurance metrics, and observation times (Mukherjee and Liu 2021; Alonso-González and Fernández-García 2021). For this analysis, we focused on the daytime LST band to capture diurnal temperature variations. The LST values, originally in Kelvin, were converted to degrees Celsius for easy interpretation and comparison. We selected 24 locations within Lagos State and one nearby area (Sango), as shown in Fig. 1. The Lagos State locations include Ikoyi, Lekki, Epe, Ikorodu, Ikeja, Mushin, Oshodi, Agege, Iyana Ipaja, Ojo, Apapa, Festac, Egbedore, Badagry, Ketu-Alapere, Yaba, Satellite Town, Akesan, Ije Ododo, Okoko, Ijegun, Ijanikin, Ajah, and Iba. Although Sango falls outside Lagos State's administrative boundary, we included it due to its close proximity and functional ties to the region. Using GEE, 8-day composite LST values were extracted for each location over the study period. To better understand long-term trends and variations, the LST data were aggregated to yearly means. This provided a clear overview of the temperature patterns for each location. In addition, the standard deviation (STD) of the yearly LST values was calculated to quantify the interannual variability to highlight areas with significant temperature fluctuations. In this study, we used daytime LST primarily because it captures peak surface temperatures, which are more indicative of heat stress and surface-atmosphere interactions during the warmest parts of the day (Malbéteau et al. 2018; Bala et al. 2020). This makes it particularly relevant for understanding thermal dynamics, land cover influence, and potential implications for heatwave.

### 2.3 Land Cover Change

To analyse land cover changes, we utilized the MODIS land cover product (MCD12Q1), which is accessible through the GEE. This dataset provides annual global land cover classifications at a spatial resolution of 500 m and categorizes land cover into 18 distinct classes, such as forests, urban

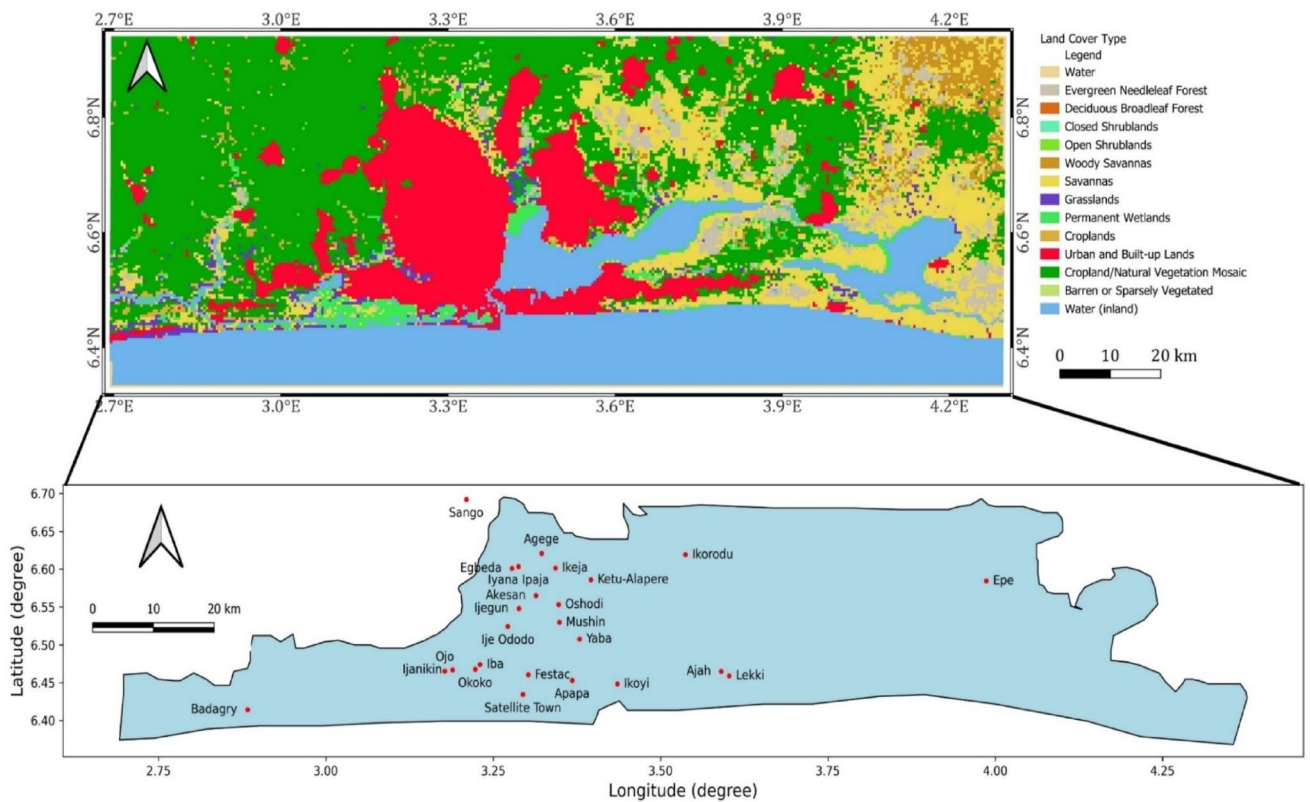


**Fig. 1** Land cover map for Lagos State as of 2020. The lower panel shows the reference locations for land surface temperature reference analysis

**Table 1** List of classification values and their corresponding land cover types

Classification value	Land cover type
0	Water
1	Evergreen Needleleaf Forest
2	Evergreen Broadleaf Forest
3	Deciduous Needleleaf Forest
4	Deciduous Broadleaf Forest
5	Mixed Forests
6	Closed Shrublands
7	Open Shrublands
8	Woody Savannas
9	Savannas
10	Grasslands
11	Permanent Wetlands
12	Croplands
13	Urban and Built-up Lands
14	Cropland/Natural Vegetation Mosaic
15	Snow and Ice
16	Barren or Sparsely Vegetated
17	Water (inland)

areas, and water bodies (Izquierdo-Verdiguier et al. 2021a, b; Khaldi et al. 2021; Kumari et al. 2024a, b). The study focused on the period between 2001 and 2020. For each year within the study period, we retrieved the first available land cover image and extracted the land cover classification

information from the *LC\_Type1 band*. These images were clipped to the Lagos region to ensure that only the relevant area was analysed, including only the pixels within the geographic boundaries of the study area. A binary mask was subsequently created for each of the 18 land cover classes defined in the MODIS dataset (represented by values of 0–17) (Table 1).

The binary mask assigned a value of 1 to pixels corresponding to a specific land cover class and 0 to all others, allowing for the isolation of individual land cover types (Izquierdo-Verdiguier et al. 2021a, b).

$$\text{Area} = \sum \text{Binary mask} \times \text{Pixel area} \quad (1)$$

where the binary mask is a raster image where the pixels of interest have a value of 1, all other pixels have a value of 0, and the pixel area is the area of each pixel in square meters.

The area occupied by each land cover class was calculated using the *pixelArea* function available in the GEE. This function computes the surface area of each pixel in square meters. To provide a more interpretable and standard unit of measurement, the computed areas were converted from  $\text{m}^2$  to  $\text{km}^2$ . For each land cover class, the total area within the study area was aggregated using the *reduceRegion* method. This method applies a sum reducer to combine the areas of

all relevant pixels, as shown in Eqs. (2) and (3) (Venkatappa et al. 2020).

$$\text{Reducer output} = \text{Reducer}(I(x, y) \text{ for all pixels } \in R) \quad (2)$$

where  $I(x, y)$  is the pixel value, and  $R$  is the region of interest. For the pixel area, the method calculates the total area of pixels with nonzero values. Thus, Eq. (2) becomes (Kumari et al. 2024a, b):

$$\text{Area} = \sum_{(x,y) \in R} [\text{mask}(x, y) \times \text{pixel area}(x, y)] \quad (3)$$

where  $\text{mask}(x, y)$  is the binary mask (1 for the pixels of interest, 0 otherwise), and  $\text{mask}(x, y)$  is the area of a single pixel (calculated based on the image scale and projection). The analyses were performed at a spatial scale of 500 m, matching the resolution of the MODIS dataset to ensure accuracy and consistency. In this analysis, only the fractions of MODIS pixels that fall within the study area were considered. Since MODIS has a spatial resolution of 500 m, some pixels extend beyond the study boundary, partially covering both inside and outside the area of interest. To ensure accuracy, the pixel area method was applied to compute only the proportion of each intersecting pixel that lies within the study area, rather than counting entire pixels that merely intersect the boundary. To understand land cover change dynamics, we conducted a temporal analysis, calculating metrics such as net change and transition matrices between different periods. Change detection techniques have also been employed to visualize the spatial patterns of land cover transformations. While the MODIS LST (1 km) and Land Cover (500 m) datasets have relatively coarse spatial resolutions, they offer significant advantages for wide-scale analysis. Their high temporal consistency, broad spatial coverage, and long-term availability make them particularly valuable for capturing large-scale environmental patterns and trends (Xu et al. 2018; Zeng et al. 2021). In this study, these strengths align well with the study's objectives. Although they may not resolve fine-scale variability, their use provides a strong foundation for understanding broader dynamics and supporting future, more detailed investigations.

### 3 Results

#### 3.1 Land Surface Temperature Analysis

The trends in the annual LST values across the 25 locations under consideration are shown in Fig. 2. Generally, the range of LST values ( $26^{\circ}\text{C} < \text{LST} < 37^{\circ}\text{C}$ ) across the

locations revealed small variations ( $11^{\circ}\text{C}$ ) in temperature within the state. The minimum values across the locations ranged from  $26.05^{\circ}\text{C}$  (Satellite Town) and  $33.87^{\circ}\text{C}$  (Agege) while the maximum values ranged from  $28.18^{\circ}\text{C}$  (Satellite Town) and  $36.5^{\circ}\text{C}$  (Oshodi). Badagry had the smallest LST range of  $1.62^{\circ}\text{C}$ , while Ikorodu had the highest LST range of  $4.56^{\circ}\text{C}$ . We observed LST values that fall within the  $21.43^{\circ}\text{C}$  to  $41.91^{\circ}\text{C}$  range reported for New Delhi (Kumari et al. 2018) and  $17\text{--}30^{\circ}\text{C}$  for Sao Paulo (do Nascimento et al. 2022). We found coastal locations such as Epe, Badagry, Ajah, and Lekki to have lower LST values than inland locations such as Mushin. This can be attributed to the effects of land-sea breezes on coastal locations and low urbanization rates. In the last 5–8 years, significant development and urbanization have occurred in Ikorodu, which can explain why the highest LST range was observed in the area. Table 2 presents the trend statistics for the annual mean LST values at the locations under consideration. The Mann–Kendall trend analysis revealed statistically significant increasing trends at 11 locations under consideration. These locations are Ajah, Egbede, Epe, Ijanikin, Ije Ododo, Ijegun, Ikorodu, Iyana Ipaja, Lekki, Ojo, and Sango.

However, there were no observable trends in the LST at the remaining locations. The Theil–Sen slope indicates the LST change rate over time. Four locations (Apapa, Badagry, Okoko, and Satellite Town) had negative trends within the period under consideration. This implies that there is cooling in the LST at rates of  $0.005$ ,  $0.017$ ,  $0.018$ , and  $0.025^{\circ}\text{C}/\text{year}$  in Okoko, Badagry, Apapa, and Satellite Town, respectively. Twenty-one locations showed an increasing trend, with rates ranging from  $0.001^{\circ}\text{C}/\text{year}$  to  $0.174^{\circ}\text{C}/\text{year}$ . We observed the lowest increase at Mushin, while the highest was at Sango. The trend values obtained in this study were lower than the global average of  $0.26\text{--}0.34^{\circ}\text{C}$  per decade from 2001 to 2020 (Wang et al. 2022) but within the  $0.02^{\circ}\text{C}/\text{year}$  and  $0.04^{\circ}\text{C}/\text{year}$  ranges from 2003 to 2017 (Liu et al. 2020). However, the trends are greater than the global average obtained using NDVI LST (Sobrino and Julien 2013) but lower than  $0.24^{\circ}\text{C}$  in Bangladesh (Imran et al. 2021).

The monthly pattern in the LST across the location is shown in Fig. 3. In Lagos State, the dry season lasts from November to March, while the wet season spans from April to October. However, the study observed a brief dry season in August (usually called August Break). A general pattern involving two peaks could be observed across the locations in the monthly LST values. These peaks are not obvious in some locations, such as Agege, Ikeja, Oshodi, and Yaba. There is an increase from January to April, which corresponds to the end of the dry season in Lagos State. From the peak in April, there was a decrease in the LST values to a minimum in July before another increase to a maximum

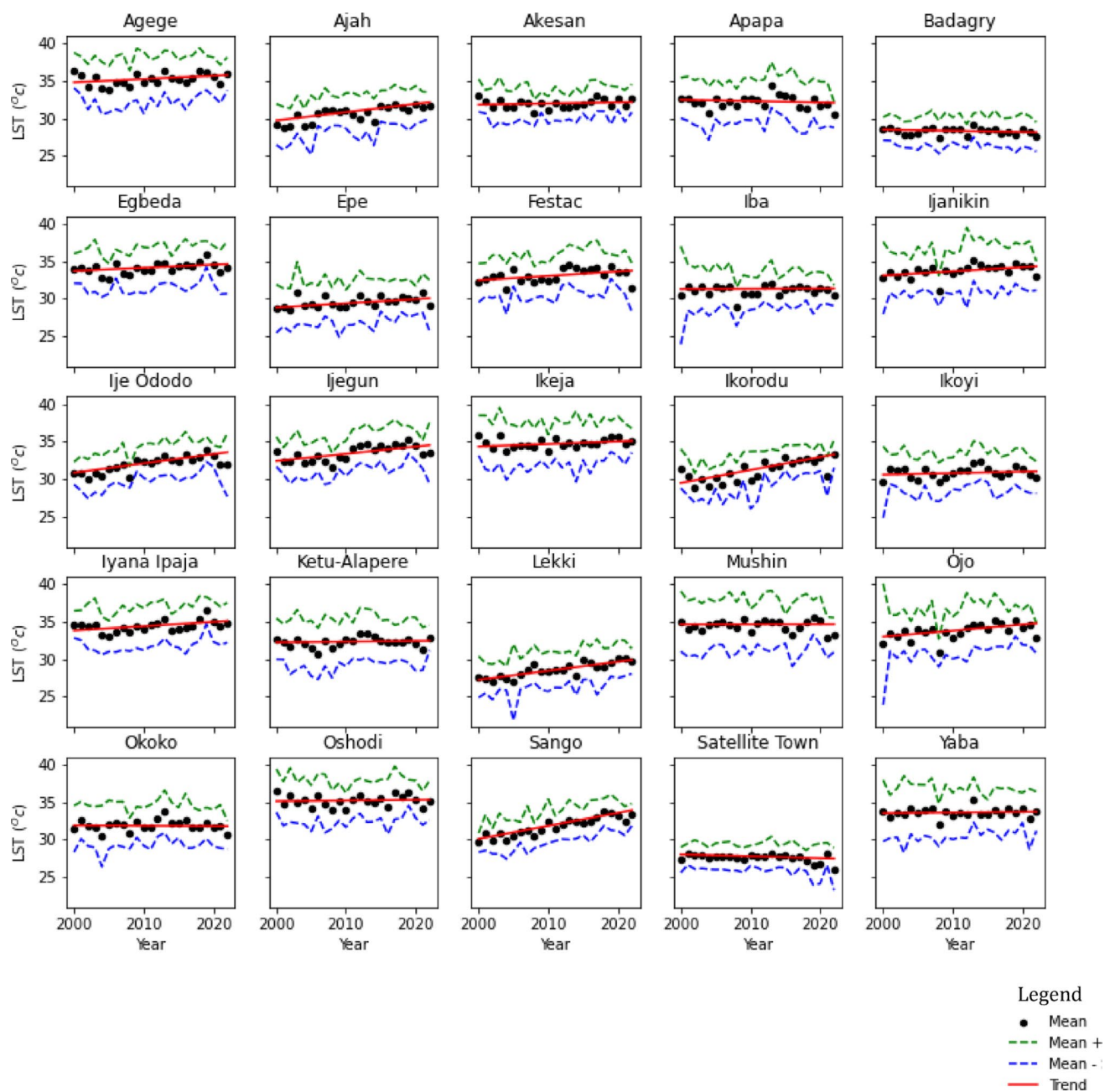


**Fig. 2** Land surface temperature time series for the reference locations

in October. From April to October, the influence of rainfall on LST values can be deduced. Land-sea breezes and the associated rainfall from April to October bring about cooling of the atmosphere and environment, thus reducing the LST. Another decrease in LST values was observed from October to December.

### 3.2 Land Cover Change Trends

#### 3.2.1 Diversity Indices

**3.2.1.1 Shannon Diversity Index** The Shannon diversity index was calculated for each year to quantify the diversity in the study area. The Shannon diversity index measures the uncertainty or unpredictability of the land cover types within a study area (Morris et al. 2014; Dowa et al. 2022). To determine the Shannon index, the total number of pixels within the study area is calculated from the land

**Table 2.** Trend statistics for the LST at the study locations

Location	MK Trend	p-value	Slope	Intercept
Agege	No trend	0.169646	0.044	34.79
Ajah	Increasing	5.96E-05	0.111	29.70
Akesan	No trend	0.369209	0.016	31.81
Apapa	No trend	0.597354	-0.018	32.47
Badagry	No trend	0.224411	-0.017	28.47
Egbeda	Increasing	0.034615	0.042	33.69
Epe	Increasing	0.015109	0.056	28.80
Festac	No trend	0.050657	0.059	32.44
Iba	No trend	0.957875	0.003	31.27
Ijanikin	Increasing	0.005118	0.056	33.08
Ije Ododo	Increasing	0.000218	0.125	30.83
Ijegun	Increasing	0.00434	0.096	32.40
Ikeja	No trend	0.224411	0.034	34.33
Ikorodu	Increasing	9.28E-05	0.173	29.46
Ikoyi	No trend	0.341718	0.020	30.57
Iyana Ipaja	Increasing	0.044729	0.057	33.85
Ketu-Alapere	No trend	0.791699	0.010	32.26
Lekki	Increasing	1.16E-05	0.121	27.25
Mushin	No trend	1.00000	0.001	34.66
Ojo	Increasing	0.00602	0.082	33.01
Okoko	No trend	0.915867	-0.005	31.90
Oshodi	No trend	0.791699	0.009	35.14
Sango	Increasing	3E-0007	0.174	30.10
Satellite Town	No trend	0.05723	-0.025	28.02
Yaba	No trend	0.711571	0.008	33.55

NB: Mann–Kendall (MK)

cover classification band (*LC\_Type1*) extracted from each MODIS image. A frequency histogram is then generated to determine the number of pixels assigned to each land cover class, and the Shannon index is computed using the Eq. (4):

$$H' = - \sum (p_i \log p_i) \quad (4)$$

where  $p_i$  is the proportion of the total pixels corresponding to each land cover class. This index shows both the number of different land cover types and their distributions within the study area. It captures the relative abundance and evenness of land cover types and the biodiversity of the area over time.

**3.2.1.2 Simpson Diversity Index** In addition to the Shannon diversity index, the Simpson diversity index was also calculated to measure the likelihood that two randomly selected pixels from the study area would belong to the same land cover class. This index enables us to assess the dominance or evenness of land cover types within the study area. The Simpson index is calculated using Eq. (5).

$$D = 1 - \sum p_i^2 \quad (5)$$

where  $p_i$  is the proportion of pixels corresponding to each land cover class. The squared terms  $p_i^2$  reflect the dominance of each land cover class, with larger values of  $p_i$  leading to a higher value for  $p_i^2$ . The sum of the squared proportions is subtracted from 1, so the index yields a value between 0 and 1. A value close to 1 indicates a high level of diversity, with multiple land cover classes being equally represented. On the other hand, a value close to 0 suggests that a few land cover classes dominate the landscape, with limited diversity. The Simpson diversity index is handy in detecting areas where a few land cover types overwhelm the landscape, providing insights into potential issues such as land degradation or monoculture practices.

As shown in Fig. 4, the Shannon index values fluctuate between 1.64 and 1.81 across the years, showing a general increasing trend from 2001 to 2015, followed by a slight decline in later years. This trend reflects significant changes in land cover diversity, particularly a decline in vegetation areas and the expansion of urban areas, as shown in Fig. 5. As shown in the figure, evergreen broadleaf forests decreased from 726.4323 m<sup>2</sup> in 2002 to 357.7694 m<sup>2</sup> in 2020, whereas open shrublands, woody savannas, and grasslands also experienced consistent declines. The observed reductions in vegetation areas reflect the impacts of land-use changes and urban encroachment on natural ecosystems. On the other hand, urban and built-up lands steadily increased, growing from 1061.903 m<sup>2</sup> in 2002 to 1818.045 m<sup>2</sup> in 2020, indicating clear evidence of urbanization. Similarly, the cropland/natural vegetation mosaic remained a dominant land cover type, peaking at 4233.341 m<sup>2</sup> in 2012. This further indicates the expansion of human-influenced landscapes. As the Shannon index indicates, these trends suggest that urban development and agricultural activities are key drivers of land cover changes, contributing to increased land cover diversity during earlier years.

The Simpson diversity index, shown in Fig. 4, measures the probability that two randomly selected pixels from the study area belong to the same land cover class. Higher index values indicate dominance by a few land cover classes, whereas lower values suggest a more balanced representation among classes (Getzin et al. 2012; Liang et al. 2015). In this study, the Simpson index values ranged from 0.74 to 0.79, emphasizing the predominance of a few land cover types, such as urban and built-up areas and cropland/natural vegetation mosaics. These are progressively displacing natural vegetation. The stable or slightly increasing Simpson index values over time indicate that urban and agricultural expansion are diminishing the presence of remaining natural vegetation, resulting in a more homogenized landscape.

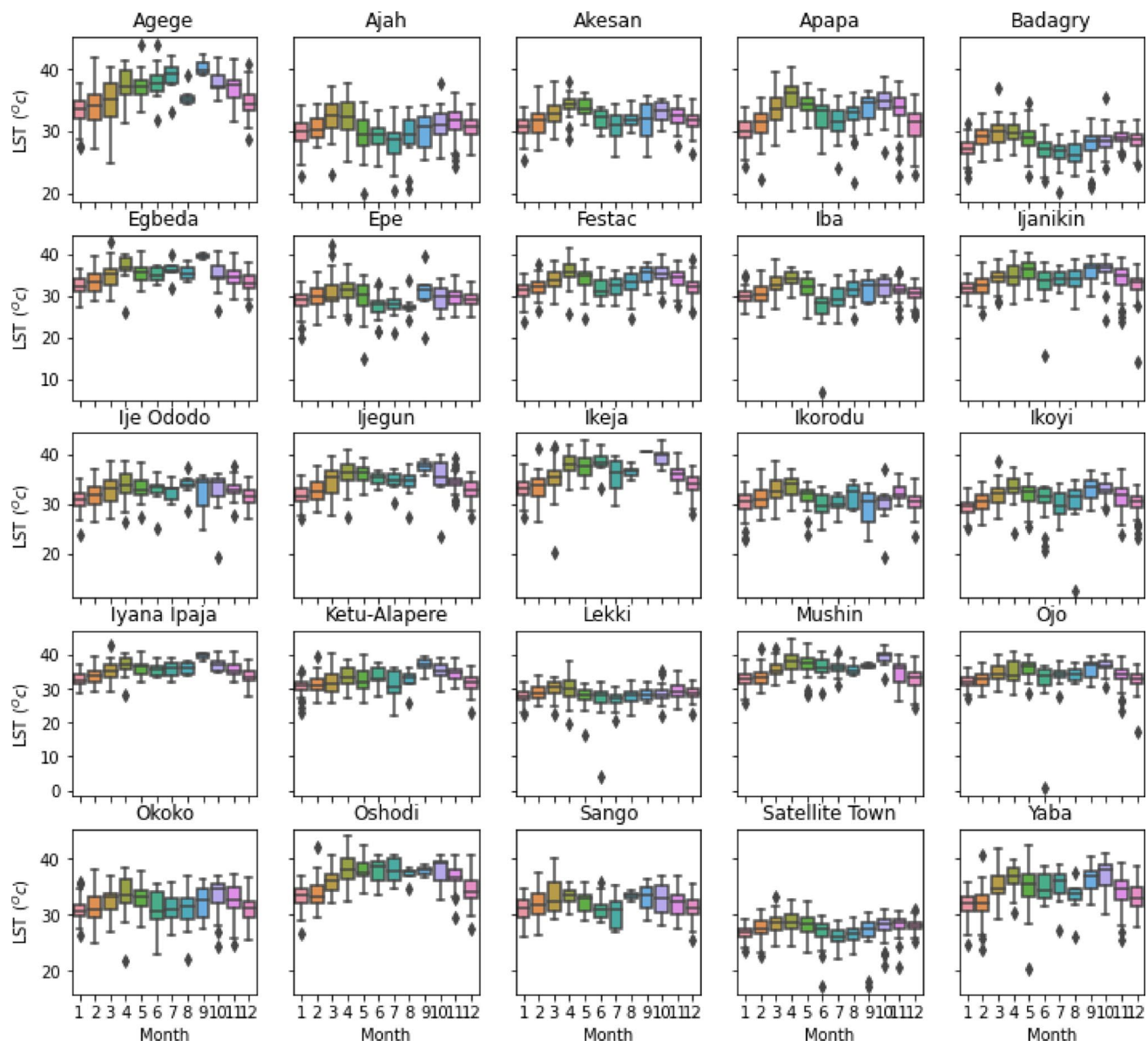


**Fig. 3** Monthly variation in LST across 25 locations in Lagos State from 2002 to 2020

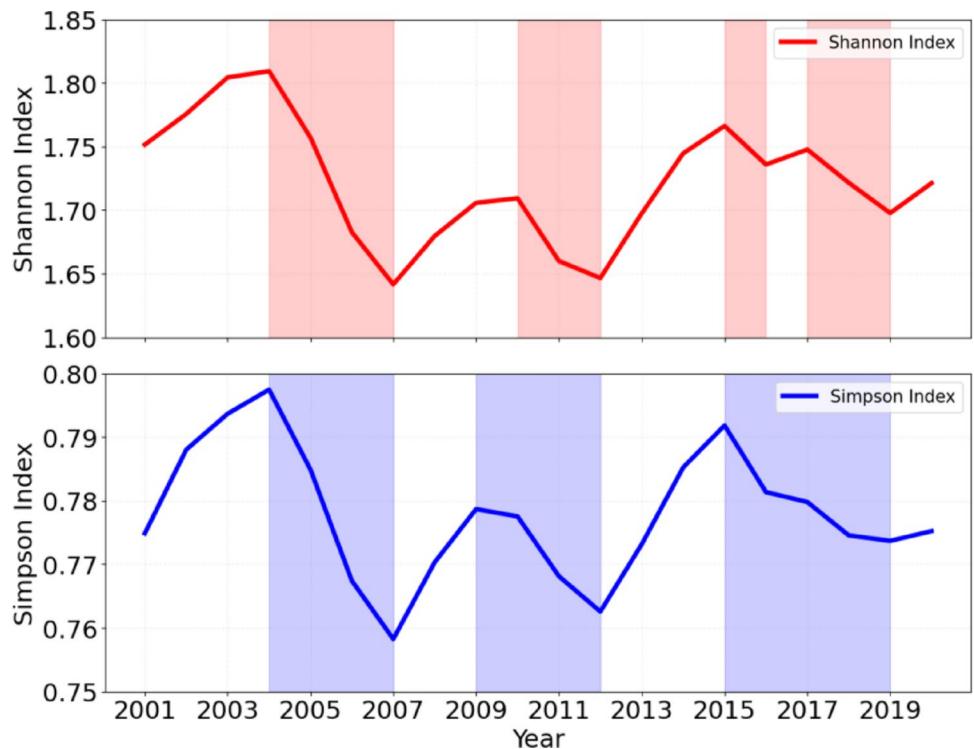
### 3.3 Changes in the Land Cover Classes

The land cover change analysis results, as shown in Fig. 5 reveal significant temporal variations in various land cover types from 2001 to 2020. These variations illustrate the dynamic processes of land use, vegetation transformation, urbanization, and natural resource utilization over the years. The evergreen broadleaf forest experienced substantial fluctuations throughout the study period. In 2002, the coverage area was 726.43 m<sup>2</sup>, representing a significant proportion of the forested area. However, by 2020, this type had diminished drastically to 357.77 m<sup>2</sup>. This continuous decline suggests deforestation and land-use change, potentially due to agricultural expansion, logging, or infrastructure

development. The peak coverage in 2010 (739.21 m<sup>2</sup>), followed by a sharp decline, may indicate episodic land restoration efforts or changes in classification accuracy during that period. Deciduous broadleaf and mixed forests remained almost negligible in coverage, with little to no coverage across most years. This indicates the dominance of evergreen species in the region or a classification preference for other types of land cover that overlap with these categories. Shrublands indicated a marked shift between the closed and open categories. Closed shrublands, which initially covered 59.05 m<sup>2</sup> in 2002, experienced significant reductions to less than 2 m<sup>2</sup> by 2020.

On the other hand, open shrublands, with minimal coverage throughout most of the years, fluctuated marginally,

**Fig. 4** Land cover diversity indices for the study area



peaking at 1.24 m<sup>2</sup> in 2017. The disappearance of closed shrublands might reflect vegetation degradation, climatic influences, or anthropogenic pressures, converting dense areas into sparser shrublands. Woody savannas and savannas underwent considerable changes. The area of woody savannas was 246.15 m<sup>2</sup> in 2002, declining significantly to 38.83 m<sup>2</sup> in 2007 but recovering to 299.82 m<sup>2</sup> by 2020. Savannas, a more extensive land cover type, initially covered 2,422.51 m<sup>2</sup> in 2002, showing a general decrease over time, ending at 1,680.82 m<sup>2</sup> in 2020. These patterns suggest shifts in vegetation density and land use, possibly influenced by grazing, fire regimes, or land conversion to agriculture. Grasslands, initially at 274.64 m<sup>2</sup>, exhibited moderate variability, peaking in 2015 at 507.95 m<sup>2</sup> before falling to 216.64 m<sup>2</sup> in 2020.

This variability could be attributed to episodic agricultural clearance, natural regrowth, or seasonal classification variations. Permanent wetlands displayed substantial inter-annual variation, with an increase from 364.01 m<sup>2</sup> in 2002 to a peak of 944.76 m<sup>2</sup> in 2004, followed by a decline to 254.73 m<sup>2</sup> in 2012 and moderate recovery to 330.46 m<sup>2</sup> by 2020. These fluctuations could reflect hydrological changes, such as rainfall patterns, river dynamics, or human interventions, such as dam construction or drainage.

However, the cropland/natural vegetation mosaic remained a dominant cover type, with slight fluctuations throughout the period. Starting at 3,655.94 m<sup>2</sup> in 2002, the coverage increased to 4,049.07 m<sup>2</sup> by 2020. This category's stability reflects its role as a transitional zone that balances agriculture and natural vegetation. Barren or sparsely

vegetated areas and inland water showed little variation over the years, with minor landscape components remaining. The barren lands remained consistently below 5 m<sup>2</sup>, whereas inland water remained steady at approximately 2,799.55 m<sup>2</sup>. This suggests minimal natural changes or human-induced impacts in these categories.

The urban and built-up areas consistently increased throughout the study period. In 2002, the area covered by urban and built-up lands was 1,061.903 m<sup>2</sup>, steadily rising to 1,818.045 m<sup>2</sup> by 2020. This represents a significant expansion of over 700 m<sup>2</sup>, or approximately 71.2%, within less than two decades. The acceleration of urbanization can likely be attributed to population growth, economic development, and the associated demand for housing, infrastructure, and urban services. This trend underscores the rapid transformation of natural and semi-natural landscapes into urban settings, driven by both migration and local population growth. Similarly, croplands have experienced a notable increase, growing from 122.4078 m<sup>2</sup> in 2002 to 174.1968 m<sup>2</sup> in 2020. This 42.3% increase reflects intensifying agricultural activities, which are often a response to the need for increased food production to support growing populations. The simultaneous expansion of croplands and urban areas suggests a relationship between these two trends, which are potentially influenced by population dynamics.

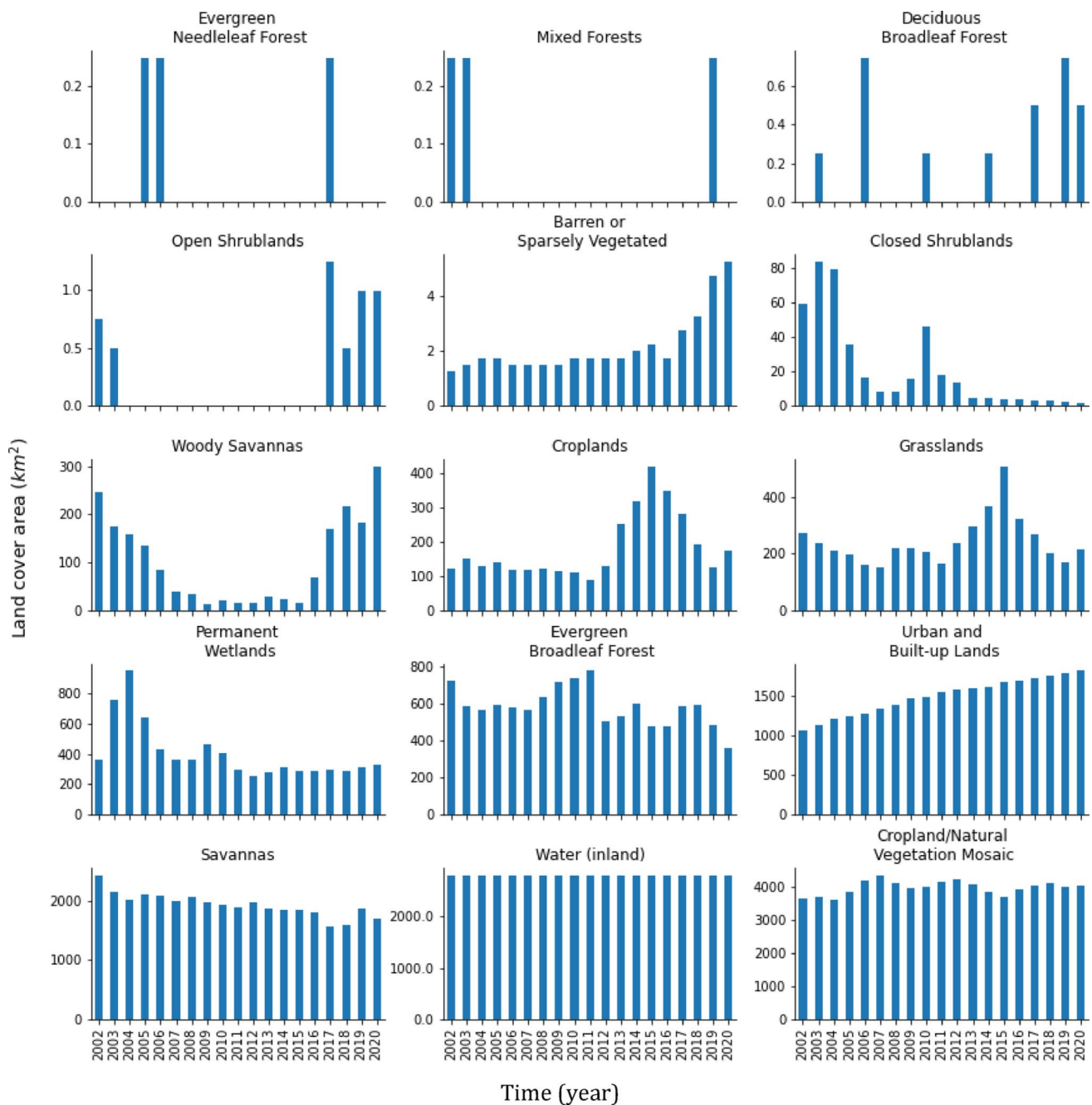


**Fig. 5** Land cover change by type (all available land cover classes in the study)

#### 4 Discussions

The compositions of the different land cover types in Lagos State are shown in Fig. 6. For the trend analysis, the various land cover types were consolidated into three broad categories: water, vegetation, and built-up land (Fig. 7). All the vegetation classes were combined under the vegetation category. As shown in Fig. 6, the area covered by vegetation experienced a continuous decline over the study period. In 2002, the vegetation cover was 7,873.38 m<sup>2</sup>, but

by 2020, it had decreased to 7,117.24 m<sup>2</sup>, representing a loss of approximately 9.6% of its original coverage. This decline is attributed to urban expansion, agricultural activities, and possibly environmental factors such as climate change and deforestation. The most notable decreases occurred between 2010 and 2020, as urban growth accelerated. Water bodies remained stable throughout the 18 years, with a consistent coverage of 2,799.55 m<sup>2</sup>. This stability suggests that water bodies were neither significantly encroached upon nor expanded during the study period, possibly because of

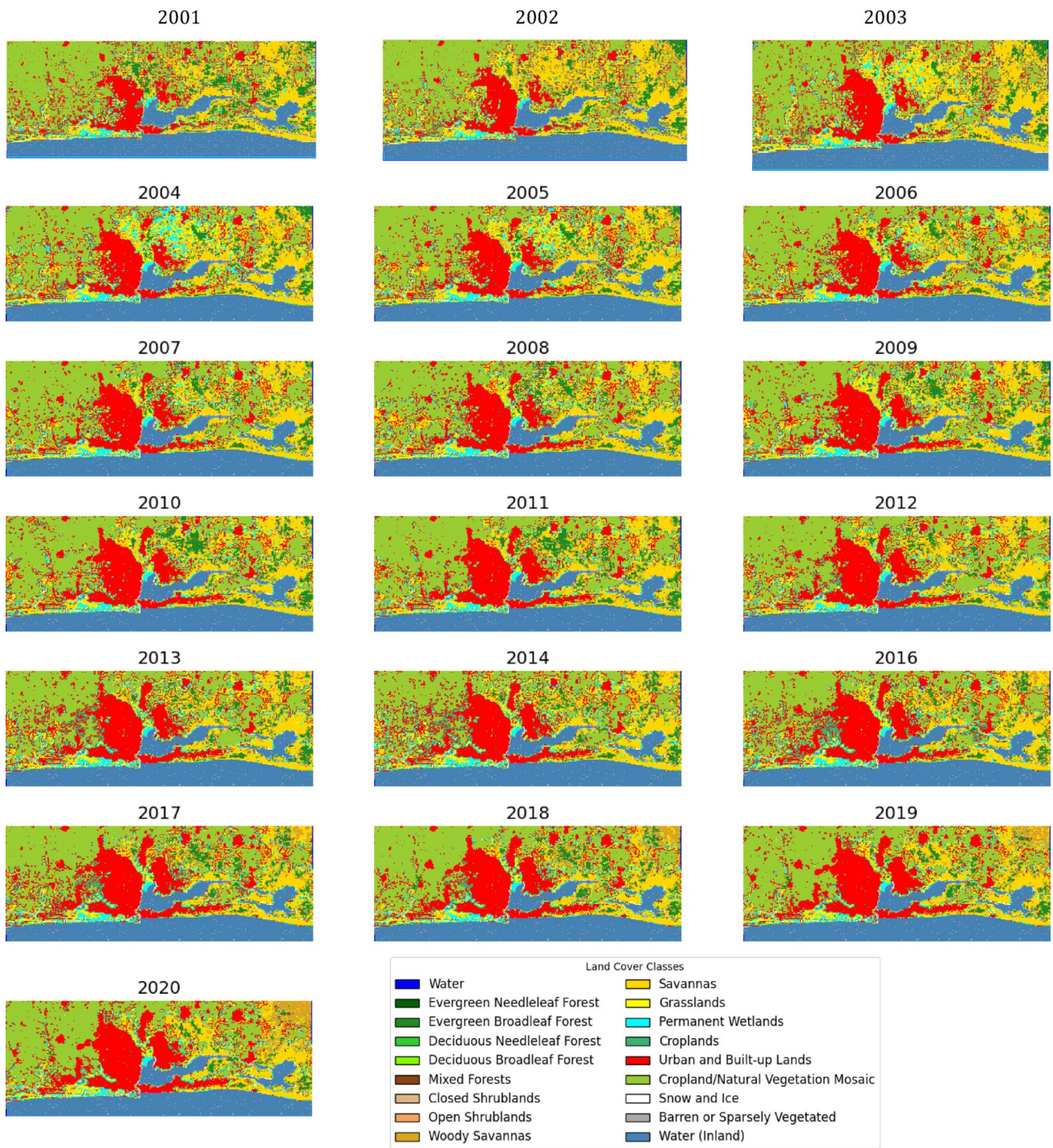


**Fig. 6** Spatial trends of various land cover types for the study area

natural boundaries or deliberate conservation efforts. On the other hand, urban and built-up lands indicated substantial growth over the same period. In 2002, the coverage of urban areas was 1,061.90 m<sup>2</sup>. By 2020, this figure had risen sharply to 1,818.04 m<sup>2</sup>, indicating an increase of 71.2%. This rapid growth reflects urbanization and infrastructure

development, likely driven by population growth, economic development, and rural-to-urban migration.

This translates to an annual loss of vegetation of over 40 m<sup>2</sup> each year. On the other hand, we observed a statistically significant increasing trend in built-up land, with a similar growth rate. As built-up areas grow, they act as hubs of consumption, driving demand for food and agricultural



**Fig. 7** Land cover change time series for three classes (water, vegetation, and urban and built-up lands)

products. This demand, in turn, may prompt the conversion of other land cover types, such as savannas or shrublands, into croplands. Moreover, urban sprawl often leads to the encroachment of built-up areas into peri-urban agricultural lands. This necessitates the creation of new cropland further away from urban centers to maintain food supply chains. This phenomenon indicates the complex trade-offs between urban development and agricultural expansion, where population growth serves as a common driver. These results reveal that the landscape has rapidly transformed due to a combination of natural processes and human activities.

The observed persistent decline in forested areas is occurring in direct contrast to the notable expansion of croplands, highlighting a significant land-use shift driven by human activities. This trend suggests that as other forest types diminish, increasingly more land is being converted into croplands to meet the growing food demands of a rising population. At the same time, urban areas continue to expand, further intensifying pressures on natural ecosystems. These interlinked patterns underscore the critical need for sustainable land management practices to mitigate the trade-offs among agricultural expansion, urban development, and ecological conservation. Lagos State is a coastal megacity with a population of more than 22 million people covering a land mass of 3577 m<sup>2</sup> (Oyalowo 2022). The city is expected to have populations of 30 million and 60 million by 2030 and 2050, respectively, with population density

expected to increase significantly soon (Enoh et al. 2023). The development of Lagos State to accommodate the present population has led to dynamic changes in land use and land cover within the state. These changes have direct and indirect effects on the atmosphere through the modulation of feedback mechanisms and changes in atmospheric cycles.

The Mann-Kendall trend analysis indicates a statistically significant decreasing trend in vegetated areas, with a loss rate exceeding 40 m<sup>2</sup> per year. This reduction in vegetation is closely associated with changes in Land Surface Temperature (LST), as illustrated in Fig. 8, which shows the relationship between LST and the Normalized Difference Vegetation Index (NDVI). For consistency in the correlation analysis, we used the overlapping period from 2001 to 2020 for both the MODIS Land LST and Land Cover datasets. While the full LST dataset spans 2000 to 2022 and the Land Cover data is available from 2001 to 2020, only the shared time frame was used in the statistical analysis to ensure methodological alignment. Specifically, our results reveal an increase in LST at 11 of the studied locations, a trend consistent with findings from similar studies in rapidly developing cities worldwide, such as those in India (Mukherjee and Singh 2020), São Paulo (do Nascimento et al. 2022), and Bangladesh (Imran et al. 2021). The rate of increase in the LST varies, with four locations showing a negative decrease and 21 locations showing a positive increase. This implies a cooling in the LST at Apapa, Badagry, Okoko,

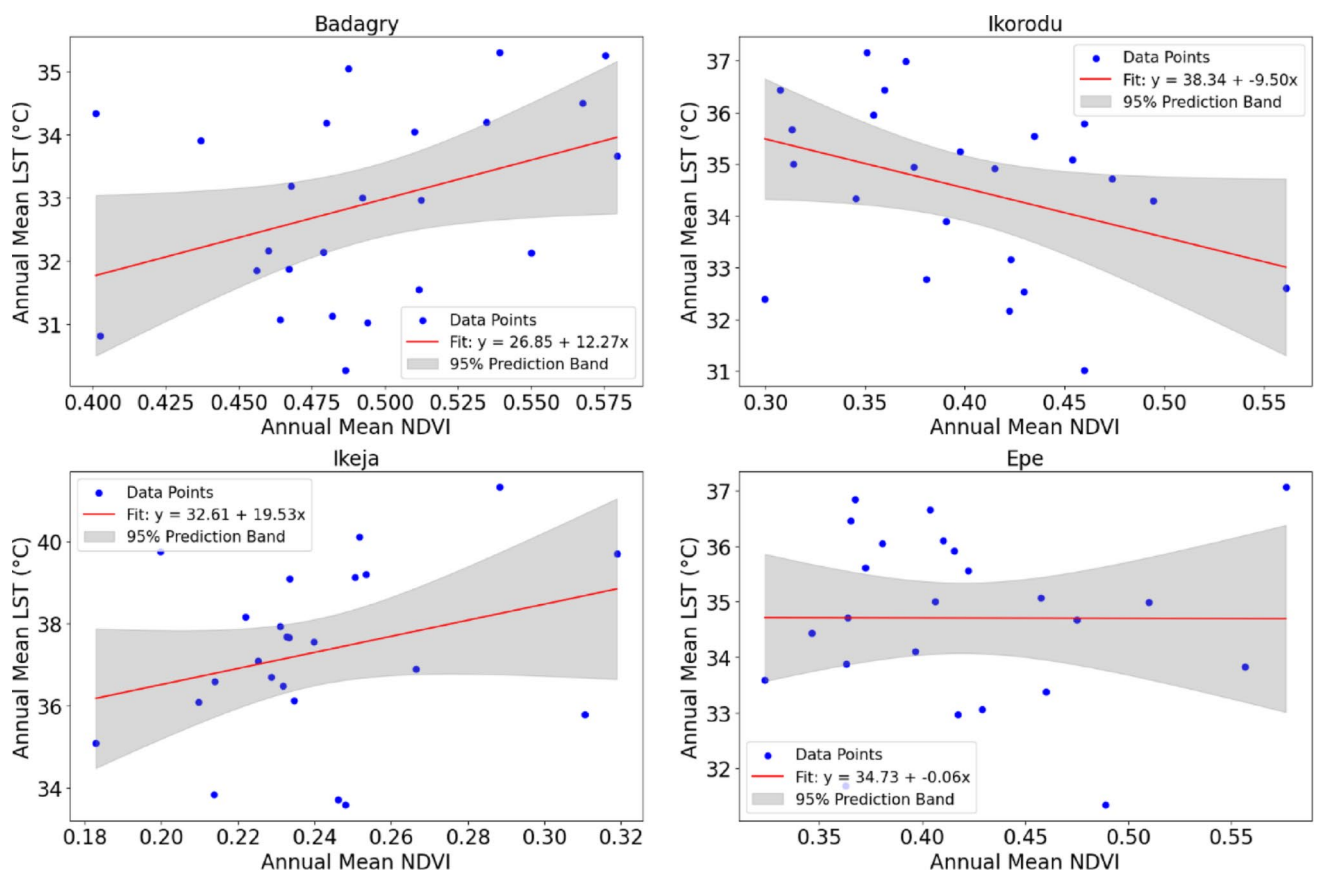


**Fig. 8** Scatter plots showing the relationship between the LST and the NDVI for some selected areas within the entire study area. The red line represents the linear regression fit with the equation displayed, while the gray shaded portion denotes the 95% confidence prediction band

and Satellite Town, whereas the other locations exhibited positive increases. A positive increase of 0.001–0.174°C/year at various locations might cause an increase in rainfall intensity (Gao et al. 2021; Lei et al. 2008), higher pollution levels (Fuladlu and Altan 2021; Huszar et al. 2020) and an increase in UHIs (Kumar et al. 2021). The combined impact of increases in rainfall intensity, pollution levels, and UHIs poses significant environmental challenges within the state. To make Lagos State inclusive, safe, resilient, and sustainable according to Sustainable Development Goal (SDG) 12, there is a need to understand the direct and remote causes of the increase in LST. The investigation of the drivers of LST will also help in the design of adaptation and mitigation strategies for impacts on cities. A study of land use and land cover within Lagos State from 2002 to 2020 using 17 classifications revealed that urbanization was the main driver. Our results showed that the rate of vegetation loss directly corresponds to the increase in urbanization in Lagos State. This implies that the urban development experienced in the last decade has come at the expense of vegetation loss. There is a need for deliberate and urgent efforts by stakeholders to incorporate vegetation development into the urban plan of the state.

## 5 Conclusion

Given the rapid urbanization and its environmental consequences, understanding how land use transformations influence temperature trends is essential for effective climate adaptation and urban planning. This study analyzed the spatiotemporal variability of LST in Lagos State and assessed the role of land cover change in shaping urban heat patterns. MODIS satellite-derived LST and land cover datasets spanning from 2002 to 2022 were utilized to achieve this. These datasets provided a high-resolution perspective on temperature variations across 25 locations within Lagos State, enabling a detailed assessment of how urban expansion and vegetation loss contribute to the observed thermal patterns. The findings reveal a significant increase in LST in 21 of the 25 study locations, with trends ranging from 0.001 °C to 0.174 °C per year. This warming pattern coincides with the expansion of built-up areas, which grew by over 71% during the study period, while vegetated areas declined at a rate of approximately 40 m<sup>2</sup> per year. The results also highlight spatial variations, with coastal locations such as Epe and Badagry exhibiting lower temperature trends than inland urban centers like Ikorodu and Sango. This suggests that

land-sea interactions may provide some moderating effects on LST, whereas intense urbanization inland amplifies heat retention. Seasonal variations further underscore the impact of rainfall and land cover, with LST peaking during the dry season and declining in the wet months due to increased atmospheric moisture and oceanic influences.

These findings align with previous studies on UHIs in rapidly developing cities. However, this study advances current knowledge by offering a more detailed spatial breakdown of temperature trends and land cover transitions within Lagos State. The results provide empirical evidence of the direct link between vegetation loss and rising temperatures, emphasizing the need for urgent interventions. While the study successfully captures long-term trends, some limitations should be acknowledged. The reliance on MODIS data, with a spatial resolution of 1 km for LST and 500 m for land cover, may overlook finer-scale variations within highly heterogeneous urban areas. Additionally, the use of 8-day composite temperature data, while effective for long-term trend analysis, may not fully capture short-term heatwave dynamics or localized temperature anomalies. Future studies integrating higher-resolution thermal imagery, ground-based measurements, and socio-economic data could provide an even more comprehensive understanding of urban heat dynamics in Lagos State. Deliberate policy actions are required to mitigate the increasing urban heat burden. Expanding urban greening initiatives, such as tree planting, green roofs, and the preservation of natural vegetation, can enhance surface cooling and reduce heat stress. Adopting reflective and cool roofing materials should be promoted to minimize heat absorption in built-up areas. Furthermore, strategic urban planning that preserves ventilation corridors can improve airflow and limit heat accumulation in densely populated zones. Given the role of excessive groundwater extraction in land subsidence, which exacerbates surface heating, integrated water management policies should be implemented to regulate borehole drilling and encourage sustainable water use. These interventions are essential for fostering climate resilience and ensuring that Lagos State remains liveable amid ongoing urbanization and climate change pressures. While this study establishes a clear link between urbanization, vegetation loss, and increased LST, it is important to note that other local factors, such as the types of built materials, intra-pixel variation in population density, and the role of aerosols or pollution, may also contribute to observed LST patterns. Due to data limitations, these factors were beyond the scope of the current analysis. However, they represent promising directions for future research that could further deepen our understanding of the complex drivers of urban thermal dynamics.

**Acknowledgements** The authors sincerely thank the Editor-in-Chief, Associate Editors, and anonymous reviewers of *Earth Systems and*

*Environment* for their invaluable feedback, which significantly improved the quality of this paper. Their constructive critiques and suggestions strengthened the clarity, rigor, and impact of our work.

**Funding** No funding received for this project.

**Data Availability** The datasets processed and analysed in this study are available from the corresponding author upon reasonable request.

## Declarations

**Conflict of interest** All authors have read, understood, and have complied as applicable with the statement on Ethical responsibilities of Authors.

## References

- Adegun O, Odunuga S, Appia Y (2015) Dynamics in the landscape and ecological services in system I drainage area of Lagos. *Ghana J Geogr* 7(1):75–96
- Adeyemi O, Shackleton CM (2023) Understanding foraging practices in Lagos metropolis to redesign urban greenspaces in support of human-nature interactions. *Urban Forestry Urban Green* 79:127805
- Ajikah LB, Adekanmbi OH, Oyebanji OO, Agboola OO, Akomaye FA, Adeonipekun PA, Ogundipe OT (2023) Floral composition and diversity of the Lagos coastal environment, South-Western, Nigeria. *Afr J Ecol* 61(1):37–47
- Alonso-González E, Fernández-García V (2021) MOSEV: a global burn severity database from MODIS (2000–2020). *Earth Syst Sci Data* 13(5):1925–1938
- Anderson GB, Bell ML (2011) Heat waves in the United States: mortality risk during heat waves and effect modification by heat wave characteristics in 43 US communities. *Environ Health Perspect* 119(2):210–218
- Auwalo FK, Bello M (2023) Exploring the contemporary challenges of urbanization and the role of sustainable urban development: a study of Lagos City, Nigeria. *J Contemp Urban Affairs* 7(1):175–188
- Bala R, Prasad R, Yadav VP (2020) A comparative analysis of day and night land surface temperature in two semi-arid cities using satellite images sampled in different seasons. *Adv Space Res* 66(2):412–425
- Bouchama A, Abuyassin B, Lehe C, Laitano O, Jay O, O'Connor FG, Leon LR (2022) Classic and exertional heatstroke. *Nat Reviews Disease Primers* 8(1):8
- Cheng J, Xu Z, Bambrick H, Prescott V, Wang N, Zhang Y, Hu W (2019) Cardiorespiratory effects of heatwaves: A systematic review and meta-analysis of global epidemiological evidence. *Environ Res* 177:108610
- Degirmenci K, Desouza KC, Fieuw W, Watson RT, Yigitcanlar T (2021) Understanding policy and technology responses in mitigating urban heat islands: A literature review and directions for future research. *Sustainable Cities Soc* 70:102873. <https://doi.org/10.1016/j.scs.2021.102873>
- Dewa DD, Buchori I, Sejati AW (2022) Assessing land use/land cover change diversity and its relation with urban dispersion using Shannon entropy in the Semarang metropolitan region, Indonesia. *Geocarto Int* 37(26):11151–11172
- Dissanayake DMSLB, Morimoto T, Murayama Y, Ranagalage M, Handayani HH (2018) Impact of urban surface characteristics and socio-economic variables on the spatial variation of land surface temperature in Lagos City. *Nigeria Sustain* 11(1):25

- do Nascimento ACL, Galvani E, Gobo JPA, Wollmann CA (2022) Comparison between air temperature and land surface temperature for the City of São Paulo. *Brazil Atmos* 13(3):491
- Emekwuru N, Ejohwomu O (2023) Temperature, humidity and air pollution relationships during a period of rainy and dry seasons in Lagos, West Africa. *Climate* 11(5):113
- Emetere ME (2019) A modified approach to estimating thermodynamic impact on buildings: A case study of poor urban setting in Lagos state. *J Eng Des Technol* 17(1):115–135
- Enoh MA, Njoku RE, Okeke UC (2023) Modeling and mapping the spatial-temporal changes in land use and land cover in Lagos: A dynamics for Building a sustainable urban City. *Adv Space Res* 72(3):694–710
- Fu KS, Allen MR, Archibald RK (2015) Evaluating the relationship between the population trends, prices, heat waves, and the demands of energy consumption in cities. *Sustainability* 7(11):15284–15301
- Fuladlu K, Altan H (2021) Examining land surface temperature and relations with the major air pollutants: A remote sensing research in case of Tehran. *Urban Clim* 39:100958
- Gadedjisso-Tossou A, Adjegan KI, Kablan AKM (2021) Rainfall and temperature trend analysis by Mann-Kendall test and significance for rainfed cereal yields in Northern Togo. *Sci* 3(1):17
- Gao Z, Zhu J, Guo Y, Luo N, Fu Y, Wang T (2021) Impact of land surface processes on a record-breaking rainfall event on May 06–07, 2017, in Guangzhou, China. *J Geophys Research: Atmos*, 126(5), e2020JD032997.
- Getzin S, Wiegand K, Schöning I (2012) Assessing biodiversity in forests using very high-resolution images and unmanned aerial vehicles. *Methods Ecol Evol* 3(2):397–404
- Guo M, Li J, He H, Xu J, Jin Y (2018) Detecting global vegetation changes using Mann-Kendall (MK) trend test for 1982–2015 time period. *Chin Geogra Sci* 28:907–919
- Guo L, Di L, Zhang C, Lin L, Chen F, Molla A (2022) Evaluating contributions of urbanization and global climate change to urban land surface temperature change: a case study in Lagos, Nigeria. *Sci Rep* 12(1):14168
- Harmay NSM, Choi M (2022) Effects of heat waves on urban warming across different urban morphologies and climate zones. *Build Environ* 209:108677
- Huszar P, Karlický J, Ďoubalová J, Nováková T, Šindelářová K, Švábik F (2020)... k, M. The impact of urban land-surface on extreme air pollution over central Europe. *Atmospheric Chemistry and Physics*, 20(20), 11655–11681
- Ikuemonisan FE, Ozebo VC (2020) Characterisation and mapping of land subsidence based on geodetic observations in Lagos, Nigeria. *Geodesy Geodyn* 11(2):151–162. <https://doi.org/10.1016/j.geog.2019.12.006>
- Ikuemonisan FE, Ozebo VC, Olatinsu OB (2020) Geostatistical evaluation of Spatial variability of land subsidence rates in Lagos, Nigeria. *Geodesy Geodyn* 11(5):316–327. <https://doi.org/10.1016/j.geog.2020.04.001>
- Imran HM, Hossain A, Islam AS, Rahman A, Bhuiyan MAE, Paul S, Alam A (2021) Impact of land cover changes on land surface temperature and human thermal comfort in Dhaka City of Bangladesh. *Earth Syst Environ* 5:667–693
- IPCC (2021) *Climate Change 2021: The Physical Science Basis. Contribution of Working Group I to the Sixth Assessment Report of the Intergovernmental Panel on Climate Change*
- Izquierdo-Verdiguier E, Moreno-Martínez Á, Adsuara JE, Muñoz-Mari J, Camps-Valls G, Moneta MP, Running SW (2021a, July) Global Upscaling of the MODIS Land Cover with Google Earth Engine and Landsat Data. In *2021 IEEE International Geoscience and Remote Sensing Symposium IGARSS* (pp. 309–312). IEEE
- Izquierdo-Verdiguier E, Moreno-Martínez Á, Adsuara JE, Muñoz-Mari J, Camps-Valls G, Moneta MP, Running SW (2021b, July) Global Upscaling of the MODIS Land Cover with Google Earth Engine and Landsat Data. In *2021 IEEE International Geoscience and Remote Sensing Symposium IGARSS*, 309–312
- Kasim OF, Wahab B, Oweniwe MF (2022) Urban expansion and enhanced flood risk in Africa: the example of Lagos. *Environ Hazards* 21(2):137–158
- Khaldi R, Alcaraz-Segura D, Guirado E, Benhammou Y, El Afia A, Herrera F, Tabik S (2021) TimeSpec4LULC: A global deep Learning-driven dataset of MODIS Terra-Aqua Multi-Spectral time series for LULC mapping and change detection. *Earth Syst Sci Data Discuss* 2021:1–28
- Kong J, Zhao Y, Carmeliet J, Lei C (2021) Urban heat Islands and its interaction with heatwaves: A review of studies on mesoscale. *Sustainability* 13(19):10923
- Kumar A, Agarwal V, Pal L, Chandniha SK, Mishra V (2021) Effect of land surface temperature on urban heat Island in Varanasi City, India. *J* 4(3):420–429
- Kumari B, Tayyab M, Shahfahad, Salman, Mallick J, Khan MF, Rahman A (2018) Satellite-driven land surface temperature (LST) using Landsat 5, 7 (TM/ETM+SLC) and Landsat 8 (OLI/TIRS) data and its association with built-up and green cover over urban Delhi, India. *Remote Sens Earth Syst Sci* 1:63–78
- Kumari A, Singh J, Gupta H (2024a) Multi-temporal analysis of vegetation extent using Google Earth engine. Natural resource monitoring, planning and management based on advanced programming. Springer Nature Singapore, Singapore, pp 29–45
- Kumari A, Singh J, Gupta H (2024b) Multi-temporal Analysis of Vegetation Extent Using Google Earth Engine. In *Natural Resource Monitoring, Planning and Management Based on Advanced Programming*, 29–45
- Laue F, Adegun OB, Ley A (2022) Heat stress adaptation within informal, low-income urban settlements in Africa. *Sustainability* 14(13):8182
- Lei M, Niyogi D, Kishtawal C, Pielke Sr RA, Beltrán-Przekurat A, Nobis TE, Vaidya SS (2008) Effect of explicit urban land surface representation on the simulation of the 26 July 2005 heavy rain event over Mumbai, India. *Atmos Chem Phys* 8(20):5975–5995
- Lemonu A, Viguerie V, Daniel M, Masson V (2015) Vulnerability to heat waves: impact of urban expansion scenarios on urban heat Island and heat stress in Paris (France). *Urban Clim* 14:586–605
- Leyk D, Hoitz J, Becker C, Glitz KJ, Nestler K, Piekarski C (2019) Health risks and interventions in exertional heat stress. *Deutsches Ärzteblatt International* 116(31–32):537
- Liang D, Zuo Y, Huang L, Zhao J, Teng L, Yang F (2015) Evaluation of the consistency of MODIS land cover product (MCD12Q1) based on Chinese 30 m GlobeLand30 datasets: A case study in Anhui Province, China. *ISPRS Int J Geo-Information* 4(4):2519–2541
- Liu J, Hagan DFT, Liu Y (2020) Global land surface temperature change (2003–2017) and its relationship with climate drivers: AIRS, MODIS, and ERA5-land based analysis. *Remote Sens* 13(1):44
- Lucas RA, Epstein Y, Kjellstrom T (2014) Excessive occupational heat exposure: a significant ergonomic challenge and health risk for current and future workers. *Extrem Physiol Med* 3:1–8
- Malbéteau Y, Parkes S, Aragon B, Rosas J, McCabe MF (2018) Capturing the diurnal cycle of land surface temperature using an unmanned aerial vehicle. *Remote Sens* 10(9):1407
- Marx W, Haunschmid R, Bornmann L (2021) Heat waves: a hot topic in climate change research. *Theoret Appl Climatol* 146(1):781–800
- McEvoy D, Ahmed I, Mullett J (2012) The impact of the 2009 heat wave on Melbourne's critical infrastructure. *Local Environ* 17(8):783–796
- Meenar M, Rahman MS, Russack J, Bauer S, Kapri K (2023) The urban poor and vulnerable are hit hardest by the heat: A heat equity Lens to understand community perceptions of climate change, urban

- heat Islands, and green infrastructure. *Land* 12(12):2174. <https://doi.org/10.3390/land12122174>
- Mensah CA (2014) Urban green spaces in Africa: nature and challenges. *Int J Ecosyst* 4(1):1–11
- Merem EC, Twumasi Y, Wesley J, Isokpehi P, Fageir S, Crisler M, Nwagboso E (2018) Analyzing emerging environmental issues in major areas: the case of Lagos in South West Nigeria. *Archit Res* 8(1):19–38
- Morris EK, Caruso T, Buscot F, Fischer M, Hancock C, Maier TS, Rillig MC (2014) Choosing and using diversity indices: insights for ecological applications from the German biodiversity exploratories. *Ecol Evol* 4(18):3514–3524
- Mukherjee R, Liu D (2021) Downscaling MODIS spectral bands using deep learning. *GIScience Remote Sens* 58(8):1300–1315
- Mukherjee F, Singh D (2020) Assessing land use–land cover change and its impact on land surface temperature using LANDSAT data: A comparison of two urban areas in India. *Earth Syst Environ* 4(2):385–407
- Nwilo PC, Olayinka DN, Obiefuna J, Atagbaza AO, Adzandeh AE (2012) Determination of land surface temperature (LST) and potential urban heat Island effect in parts of Lagos state using satellite imageries. *FUTY J Environ* 7(1):19–33
- Obe OB, Morakinyo TE, Mills G (2023) Assessing heat risk in a sub-saharan African humid City, Lagos, Nigeria, using numerical modelling and open-source Geospatial socio-demographic datasets. *City Environ Interact* 20:100128
- Obiefuna JN, Nwilo PC, Okolie CJ, Emmanuel EI, Daramola OE (2018) Dynamics of land surface temperature in response to land cover changes in Lagos metropolis. *Nigerian J Environ Sci Technol* 2(2):148–159
- Ogunjo ST, Akinsusi JO, Fuwape IA (2021) February Trends in extreme temperature indices over Lagos, Nigeria. In *IOP Conference Series: Earth and Environmental Science* (Vol. 655, No. 1, p. 012003). IOP Publishing
- Ogunjo ST, Adesiji N, Ojeyemi N (2023) November Heatwave trends in Lagos state, Nigeria. In *AIP Conference Proceedings* (Vol. 3040, No. 1). AIP Publishing
- Ojeh VN, Balogun AA, Okhimamhe AA (2016) Urban-rural temperature differences in Lagos. *Climate* 4(2):29
- Okuneye PA, Adebayo K, Opeolu BT, Baddru FI (2016) *Analysis of the Interplay of Migration and Urban Expansion, on Health and the Environment: The Case of Lagos, Nigeria* (Doctoral dissertation, Thesis, Committee for International Cooperation in National Research in Demography)
- Opoko AP, Oluwatayo A (2014) Trends in urbanisation: implication for planning and low-income housing delivery in Lagos, Nigeria. *Archit Res* 4(1A):15–26
- Osho GS, Ojumu O (2024) A critical investigation of Lagos state socioeconomic and economic challenges: does urban growth policy matter in Nigeria? *J Appl Bus Econ*, 26(2)
- Oyalowo B (2022) Implications of urban expansion: land, planning and housing in Lagos. *Build Cities* 3(1):692–708
- Ren Z, Wang C, Guo Y, Hong S, Zhang P, Ma Z, Meng F (2024) The cooling capacity of urban vegetation and its driving force under extreme hot weather: A comparative study between dry-hot and humid-hot cities. *Build Environ* 263:111901
- Smith TT, Zaitchik BF, Gohlke JM (2013) Heat waves in the united States: definitions, patterns and trends. *Clim Change* 118:811–825
- Sobrino JA, Julien Y (2013) Trend analysis of global MODIS-Terra vegetation indices and land surface temperature between 2000 and 2011. *IEEE J Sel Top Appl Earth Observations Remote Sens* 6(5):2139–2145
- Sojobi AO, Balogun II, Salami AW (2016) Climate change in Lagos State, Nigeria: what really changed? *Environ Monit Assess* 188:1–42
- Speak AF, Rothwell JJ, Lindley SJ, Smith CL (2013) Reduction of the urban cooling effects of an intensive green roof due to vegetation damage. *Urban Clim* 3:40–55
- UN-Habitat (2020) World cities report 2020: the value of sustainable urbanization. United Nations Human Settlements Programme (UN-Habitat)
- United Nations (UN) (2019) The sustainable development goals report 2019. United Nations, New York
- Venkatappa M, Sasaki N, Anantsuksomsri S, Smith B (2020) Applications of the Google Earth engine and phenology-based threshold classification method for mapping forest cover and carbon stock changes in Siem reap Province, Cambodia. *Remote Sens* 12(18):3110
- Wang YR, Hessen DO, Samset BH, Stordal F (2022) Evaluating global and regional land warming trends in the past decades with both MODIS and ERA5-Land land surface temperature data. *Remote Sens Environ* 280:113181
- Wehrli K, Guillod BP, Hauser M, Leclair M, Seneviratne SI (2019) Identifying key driving processes of major recent heat waves. *J Geophys Research: Atmos* 124(22):11746–11765
- World Health Organization (2021) Heat and health in the WHO European Region: updated evidence for effective prevention
- Xu B, Park T, Yan K, Chen C, Zeng Y, Song W, Myneni RB (2018) Analysis of global LAI/FPAR products from VIIRS and MODIS sensors for spatio-temporal consistency and uncertainty from 2012–2016. *Forests* 9(2):73
- Zeng L, Wardlow BD, Hu S, Zhang X, Zhou G, Peng G, Wu W (2021) A novel strategy to reconstruct NDVI time-series with high Temporal resolution from MODIS multi-temporal composite products. *Remote Sens* 13(7):1397
- Zhao L, Oppenheimer M, Zhu Q, Baldwin JW, Ebi KL, Bou-Zeid E, Liu X (2018) Interactions between urban heat Islands and heat waves. *Environ Res Lett* 13(3):034003
- Zou Z, Yan C, Yu L, Jiang X, Ding J, Qin L, Qiu G (2021) Impacts of land use/land cover types on interactions between urban heat Island effects and heat waves. *Build Environ* 204:108138
- Zuo J, Pullen S, Palmer J, Bennetts H, Chileshe N, Ma T (2015) Impacts of heat waves and corresponding measures: a review. *J Clean Prod* 92:1–12

**Publisher's Note** Springer Nature remains neutral with regard to jurisdictional claims in published maps and institutional affiliations.

Springer Nature or its licensor (e.g. a society or other partner) holds exclusive rights to this article under a publishing agreement with the author(s) or other rightsholder(s); author self-archiving of the accepted manuscript version of this article is solely governed by the terms of such publishing agreement and applicable law.